Published in final edited form as:
Cell Metab. 2014 February 4; 19(2): 232–245. doi:10.1016/j.cmet.2013.12.013.

A Redox-Dependent Mechanism for Regulation of AMPK Activation by Thioredoxin1 during Energy Starvation

Dan Shao[1], **Shin-ichi Oka**[1], **Tong Liu**[2], **Peiyong Zhai**[1], **Tetsuro Ago**[1], **Sebastiano Sciarretta**[1], **Hong Li**[2], and **Junichi Sadoshima**[1,*]

[1]Department of Cell Biology and Molecular Medicine, Cardiovascular Research Institute, New Jersey Medical School, Rutgers Biomedical and Health Sciences, Newark, NJ 07103, USA

[2]Center for Advanced Proteomics Research and Department of Biochemistry and Molecular Biology, New Jersey Medical School Cancer Center, Rutgers Biomedical and Health Sciences, Newark, NJ 07103, USA

Summary

5'-AMP-activated protein kinase (AMPK) is a key regulator of metabolism and survival during energy stress. Dysregulation of AMPK is strongly associated with oxidative stress-related disease. However, whether and how AMPK is regulated by intracellular redox status remains unknown. Here we show that the activity of AMPK is negatively regulated by oxidation of Cys130 and Cys174 in its a subunit, which interferes with the interaction between AMPK and AMPK kinases (AMPKK). Reduction of Cys130/Cys174 is essential for activation of AMPK during energy starvation. Thioredoxin1 (Trx1), an important reducing enzyme that cleaves disulfides in proteins, prevents AMPK oxidation, serving as an essential cofactor for AMPK activation. High-fat diet consumption downregulates Trx1 and induces AMPK oxidation, which enhances cardiomyocyte death during myocardial ischemia. Thus, Trx1 modulates activation of the cardioprotective AMPK pathway during ischemia, functionally linking oxidative stress and metabolism in the heart.

Introduction

Reactive oxygen species (ROS) are continuously generated by cells to regulate cellular responses such as proliferation, differentiation, and apoptosis (Finkel, 2003). ROS modulate signaling molecules through reversible post-translational reductive and oxidative modification of protein structures. Specific cysteine thiol groups (R-SH) are oxidized to sulfenic acid (R-SOH), followed by rapid interaction with other protein thiol groups to form disulfide bonds. Disulfide bond formation within redox-sensitive proteins regulates subcellular localization, protein-protein interactions, and protein structure, thereby regulating their functional activity. Sulfenic acid is vulnerable to further, largely irreversible, oxidation, forming either sulfinic acid ($R\text{-}SO_2^{-2}$) or sulfonic acid ($R\text{-}SO_3^{-2}$) (Berndt et al., 2007). Excess ROS generation, termed oxidative stress, is involved in the pathogenesis of various diseases, such as cardiovascular disease, neurodegenerative disease, and

*Correspondence: Junichi Sadoshima, MD PhD Department of Cell Biology and Molecular Medicine New Jersey Medical School Rutgers, The State University of New Jersey 185 South Orange Ave., MSB G609 Newark, NJ 07103 Tel: (973)972-8619 Fax: (973)972-8919 sadoshju@njms.rutgers.edu.

inflammation. However, under physiological conditions, excess ROS are usually removed by scavenging systems such as thioredoxin (Trx) and glutathione (Berndt et al., 2007).

Mammalian Trx1 contains a common disulfide active motif, Cys-Gly-Pro-Cys. Trx1 catalyzes disulfide reduction through a thiol disulfide exchange reaction involving Cys32 and Cys35 in its active site, leaving the target protein reduced and Trx1 oxidized (Kallis and Holmgren, 1980). Oxidized Trx1 is reduced and regenerated by Trx1 reductase (Trx1R) using electrons from NADPH (Mustacich and Powis, 2000). Trx1 acts both as a major disulfide reductase, thereby maintaining the cellular thiol redox homeostasis, and as a modulator of transcription factors and kinases, regulating their activities in a redox-dependent manner (Lillig and Holmgren, 2007).

ROS, produced by mitochondrial leakage and other enzymatic sources, are associated with cardiovascular diseases. Trx1 activity is essential for reducing oxidative stress, inhibiting cardiac hypertrophy and attenuating cardiac cell death (Ago et al., 2008). Trx1 not only maintains the intracellular redox balance by regenerating active peroxiredoxin but also acts as a signaling molecule to transduce signals to other effectors. For example, Trx1 inhibits apoptosis by negatively regulating apoptosis signal-regulating kinase (ASK1) and Ras in cardiomyocytes (Kuster et al., 2005; Saitoh et al., 1998) and prevents cardiac hypertrophy by reducing Class II histone deacetylases (HDACs) and inhibiting their nuclear export (Ago et al., 2008). Identification of the molecular targets of Trx1 is therefore an important step in understanding the key signaling events mediating cardiovascular pathogenesis.

Using unbiased proteomic approaches, we showed that Trx1 reduces proteins involved in cardiac energy dynamics (Fu et al., 2009). Trx1 also plays an important protective role during ischemia and reperfusion, which cause energy stress and eventual cell death in the heart (Tao et al., 2004). We predict that Trx1 protects the heart by reducing critical molecules involved in energy/metabolism. Currently, however, functionally relevant targets of Trx1 during myocardial ischemia are unknown.

During myocardial ischemia, the low-energy sensor, 5'-AMP-activated protein kinase (AMPK), is activated and stimulates adaptive mechanisms to restore the cellular energy conditions (Russell et al., 2004). AMPK activity is tightly regulated at Thr172 in its activation segment by phosphorylation by AMPK kinases (AMPKKs) or allosteric prevention of dephosphorylation when high levels of AMP or ADP bind to the γ subunit (Hawley et al., 1996; Oakhill et al., 2011). Due to its master role in controlling both cellular and whole-body metabolic responses, AMPK is becoming a promising therapeutic target for insulin resistance, type 2 diabetes, metabolic syndrome, and obesity, all energy balance disorders (Hardie, 2008). Complications of these metabolic disorders, which occur more frequently with aging, are associated with chronic ROS accumulation and correlate with insensitivity of AMPK activation to various stimuli (Reznick et al., 2007; Sciarretta et al., 2012; Sriwijitkamol et al., 2007). However, whether direct post-translational oxidative modification affects AMPK activity during metabolic stress is currently unknown.

Using mice harboring a Trx1 substrate-trapping mutant, we identified AMPKα as a target of Trx1 that is critical to cardiac protection against ischemia. During myocardial ischemia, oxidation of Cys130 and Cys174 causes aggregation of AMPK through intermolecular disulfide bond formation, which prevents phosphorylation/activation of AMPK by upstream AMPKKs. However, endogenous Trx1 prevents this oxidation in response to oxidative stimulus. High-fat diet (HFD) consumption decreased Trx1 expression and increased AMPK oxidation, enhancing susceptibility to myocardial infarction. Thus, AMPK activation is critically regulated by intracellular redox status and Trx1 acts as an essential co-factor,

allowing AMPK activation to occur during energy stress by preventing oxidative aggregation.

Results

AMPK Is a Direct Target of Trx1

Mutation of Cys35 in the catalytic center to serine (C35S) allows Trx1 to trap its substrates by preventing completion of the thiol disulfide exchange reaction (Figure 1A) (Verdoucq et al., 1999). In order to identify cardiac Trx1 targets *in vivo*, we generated transgenic mice with cardiac-specific expression of epitope (N-terminal FLAG and C-terminal HA)-tagged Trx1C35S (Tg-Trx1C35S). Three lines of transgenic mice were generated and the one with the lowest transgene expression (line 1, Figure S1A) was used in further experiments. All three lines exhibited apparently normal baseline cardiac phenotypes, including heart weight/body weight, an index of cardiac hypertrophy (Figure S1B). To examine the role of Trx1 during energy starvation *in vivo*, mice were subjected to myocardial ischemia and the extent of myocardial infarction was evaluated. Transgenic mice with cardiac-specific overexpression of Trx1 (Tg-Trx1) exhibited significantly less myocardial infarction, whereas Tg-Trx1C35S mice and transgenic mice with cardiac-specific overexpression of a dominant negative Trx1 mutant (C32S/C35S) (Tg-Trx1C32S/C35S) had significantly more infarction than wild type (WT) mice after 3 hours of ischemia (Figure 1B). The percentage of Hairpin-2 positive nuclei, indicating necrotic cell death, was significantly lower in Tg-Trx1, but higher in Tg-Trx1C35S and Tg-Trx1C32S/C35S, than in WT mice after ischemia (Figure S1C). These data suggest that the Trx1 thiol disulfide exchange reaction protects the heart against prolonged ischemia.

To identify the Trx1 substrates involved in this cardioprotection, heart homogenates were prepared from WT and Tg-Trx1C35S mice, and proteins that form a disulfide bond with Cys32 of Trx1C35S were co-precipitated with a FLAG antibody and analyzed by immunoblot. *N*-Ethylmaleimide (NEM) (20 mM) was added to the lysis buffer to block free thiol groups and prevent spontaneous cysteine oxidation during protein sample extraction, which can lead to non-specific capture by the Trx1 trapping mutant. Peroxiredoxin, a well-known Trx1 target, was one of the proteins identified through this analysis (Figure S1D), confirming the efficacy of the trapping mutant *in vivo*. Of the proteins identified (Figure 1C and S1D and Table S1), we focused on the AMPK α subunit because of its importance in protecting the heart against ischemic injury (Russell et al., 2004) and the absence of prior evidence that thiol disulfide exchange is involved in its regulation.

Endogenous AMPKα and Trx1 were present in both cytosol and nucleus in cardiomyocytes (Figure 2A and 2B), and they interacted with one another in both cardiomyocytes *in vitro* and the heart *in vivo* (Figure 2C). To determine whether AMPKα forms a disulfide bond with Trx1, their interaction was examined after mutation of the Trx1 active site. H_2O_2 enhanced interaction of AMPKα with Trx1C35S but not with WT Trx1 or Trx1C32S/C35S (Figure 2D). The interaction between Trx1C35S and AMPKα was almost completely abolished by addition of dithiothreitol (DTT), a reducing agent that cleaves disulfide bonds (Figure 2E). These results suggest that AMPKα and Trx1 interact at baseline and that oxidative stress further stimulates disulfide bond formation between AMPKα and Cys32 in Trx1C35S. The expected increase in intermolecular disulfide bond formation between AMPKα and WT Trx1 in response to H_2O_2 was not apparent due to completion of the thiol disulfide exchange reaction via the reduced Cys35 in WT Trx1. Overexpression of WT Trx1, but not C35S or C32S/C35S mutants, prevented AMPK inactivation in response to H_2O_2 (Figure S2A), indicating that the enzymatic activity of Trx1 is required to maintain AMPK activity in the presence of oxidative stress.

Phosphorylation of AMPKα and its substrate Acetyl-CoA carboxylase (ACC) was increased in the ischemic heart. However, the increase in phosphorylation was abolished in Tg-Trx1C35S and Tg-Trx1C32S/C35S mice (Figure 2F and S2B), suggesting that the oxidoreductase activity of Trx1 is required for ischemia-induced AMPK activation *in vivo*.

Trx1 Acts as a Co-factor of AMPK in Response to Energy Stress

An adenovirus harboring Trx1 short hairpin RNA (Ad-sh-Trx1) significantly inhibited glucose deprivation (GD)-induced phosphorylation of both AMPKα and ACC in cardiomyocytes (Figure 3A), indicating that endogenous Trx1 plays an essential role in mediating AMPK activation *in vitro*.

AMPK activation during energy stress induces translocation of glucose transporter 4 (Glut4), which in turn stimulates glycolysis in cardiomyocytes (Russell et al., 2004). Immunostaining and immunoblot analyses of the membrane fraction showed that Trx1 downregulation disrupted GD-induced Glut4 translocation to the plasma membrane (Figure 3B and S3A). GD-induced phosphorylation of phosphofructokinase 2 (PFK-2) and increases in the glycolysis rate were also attenuated in Ad-sh-Trx1-treated cardiomyocytes (Figure 3C). GD-induced decreases in ATP content and cell survival were exacerbated in cardiomyocytes treated with Ad-sh-Trx1 compared to in those with Ad-sh-scramble (Figure 3D and S3B). This effect was similar to that observed with dominant negative AMPK adenovirus (Ad-dn-AMPK) (Figure 3D and S3B). Suppression of AMPK in the presence of Trx1 downregulation did not further increase GD-induced cell death (Figure 3D). On the other hand, overexpression of either AMPK or Trx1 prevented GD-induced cell death (Figure S3C and S3D). Together, these data suggest that Trx1 plays an essential role in mediating AMPK activation and adaptive responses during GD.

Interestingly, both GD and 5-amino-1-β-Dffff-ribofuranosyl-imidazole-4-carboxamide (AICAR), which activates AMPK, also upregulated Trx1, an effect that was abolished in the presence of Ad-dn-AMPK (Figure S3E and S3F). Thus, AMPK activation is necessary and sufficient for Trx1 upregulation, suggesting that AMPK and Trx1 coordinately regulate each other during energy stress.

Trx1 Prevents Oxidation of AMPK in Response to Energy Stress

Since the oxidoreductive activity of Trx1 is required for AMPK activation during energy stress, we hypothesized that AMPKα undergoes oxidative modification. GD significantly induced H_2O_2 production, as evaluated with CM-H_2DCFDA staining (Figure S4A). In order to examine whether AMPKα exhibits an electrophoretic mobility shift indicative of oxidative modification in response to energy stress, cardiomyocytes were incubated with glucose-free medium. Cardiomyocytes were also treated with H_2O_2 as an exogenous oxidant to examine oxidation of AMPK. Cell lysates were separated by SDS-PAGE under non-reducing conditions in the absence of β-mercaptoethanol (βME). Duplicate samples were run on 6% and 8% gels in order to separate both high and low molecular weight proteins reactive with the AMPKα antibody (Figure S4B). Immunoblot analyses revealed that AMPKα shifted to high molecular weights and monomeric AMPKα was decreased in GD- or H_2O_2-treated myocytes (Figure 4A and 4B). βME abolished these mobility shifts, suggesting that the slow-migrating AMPKα immunoreactive complex most likely represents oxidative aggregation caused by disulfide bond formation (Figure 4A and 4B). Trx1 downregulation significantly weakened the monomer and increased the shift of AMPKα to higher molecular weights during GD or H_2O_2 treatment (Figure 4A and 4B), suggesting that endogenous Trx1 is essential in preventing AMPKα oxidation. Increased oxidative aggregation and decreased monomeric AMPKα were also observed in ischemic hearts (Figure S4C), suggesting AMPKα disulfide bond formation *in vivo*. Electrophoresis of

recombinant AMPKα2, the predominant α subunit in the heart, also revealed a mobility shift that was dose-dependently exacerbated by H_2O_2 (Figure 4C), indicating that cysteine oxidation in the α subunit is sufficient for aggregate formation. Consistent with the biochemical data, immunofluorescent staining with AMPKα antibody revealed a punctate pattern indicative of AMPKα aggregation after H_2O_2 treatment (Figure 4D). Together, these results suggest that Trx1 inhibits disulfide bond formation in AMPKα during energy stress.

To evaluate the redox status of cysteines in AMPKα, pull-down assays were performed with biotinylated iodoacetamide (IAM). IAM covalently binds to cysteine thiol groups only when they are in the reduced form. With increasing concentrations of H_2O_2, the amount of IAM-labeled AMPKα decreased significantly (Figure 4E). However, overexpression of Trx1 maintained the amount of reduced form AMPKα even in the presence of H_2O_2 (10 μM) (Figure S4D). These data indicate that AMPKα contains redox-sensitive cysteines that are rapidly oxidized during oxidative stress and can be reduced by Trx1. Although H_2O_2 did not significantly affect basal AMPKα Thr172 phosphorylation, it dose-dependently suppressed AICAR-induced phosphorylation and activation of AMPK (Figure S4E–S4H). Thus, cysteine oxidation blocks AICAR-induced AMPK activation, mimicking the effect of Trx1 downregulation during energy starvation. High dosage (300 μM) H_2O_2 inhibited AMPK activity in cardiomyocytes even at baseline (Figure S4I) and caused strong oxidative aggregation of AMPK (Figure S4J). In contrast, the same dose of H_2O_2 induced AMPK activation in HEK 293 cells (Figure S4I), consistent with previous findings (Zmijewski et al., 2010). There was no AMPK aggregation or decrease in monomeric AMPK in the presence of H_2O_2 in HEK 293 cells (Figure S4J), suggesting that oxidative aggregation and the amount of monomeric/reduced AMPK critically regulate AMPK activity in both cell types.

To test whether AMPKα oxidation is reversible, cardiomyocytes were sequentially treated with H_2O_2 and normal medium. After removal of H_2O_2, reduced form AMPKα reappeared and reverted to normal levels (Figure 4F). To evaluate the relative importance of Trx1 and glutathione (GSH), which also mediates protein disulfide reduction, in reduction of oxidized AMPK, we preincubated cardiomyocytes with either buthioninesulfoximine (BSO), an inhibitor of GSH synthesis, or 2,4-dinitro-1-chlorobenzene (DNCB), which prevents Trx recycling by inhibiting TrxR (Arner et al., 1995). BSO decreased the GSH level by about 60%, whereas DMSO and DNCB did not (Figure S4K). DNCB completely prevented reduction and further enhanced oxidation of AMPKα upon removal of H_2O_2, whereas DMSO (vehicle) and BSO had no effect (Figure 4F). Thus, AMPKα oxidation is reversible and Trx1, but not GSH, is required to reduce the oxidized AMPKα in cardiomyocytes.

Conserved AMPKα Cysteines Are Oxidized

Next, we investigated which AMPKα cysteine is sensitive to oxidation. Amino acid sequence alignment showed that Cys130 and Cys174 are the only two cysteines that are completely conserved from yeast to mammals (Figure 5A). To identify redox-sensitive cysteines, recombinant AMPKα2 was treated with or without 10 μM H_2O_2 for 10 minutes. Reduced cysteines were then irreversibly labeled with IAM, whereas oxidized cysteines were first reduced with DTT and then labeled with S-Methyl methanethiosulfonate (MMTS). Tandem mass spectrometry (MS/MS) showed that a peptide containing Cys174 of AMPKα2 existed predominantly in an IAM-labeled (reduced) form in the control group but that an MMTS-labeled (oxidized) form appeared in the H_2O_2-treated group (Figure 5B), suggesting that Cys174 is oxidized in response to H_2O_2. Cys130 and Cys490 were also oxidized in response to H_2O_2 (Figure S5A and S5B). At high doses of H_2O_2, Cys297, Cys382 and Cys543 were also found to be oxidized (data not shown), suggesting that more cysteines within the AMPKα2 subunit may be oxidized in the presence of severe oxidative stress.

We examined whether Cys130 or Cys174 is involved in the interaction with the catalytic motif of Trx1. As expected, the interaction between WT AMPKα2 and Trx1C35S was enhanced in the presence of H_2O_2 (Figure 5C). A single mutation to serine at Cys130 (AMPKC130S) or Cys174 (AMPKC174S) did not abolish the H_2O_2-induced increase in interaction between AMPKα2 and Trx1C35S (Figure 5C left panel). However, mutation of both Cys130 and Cys174 to serine (AMPK2CS) did inhibit the H_2O_2-induced increase in interaction with Trx1C35S (Figure 5C right panel). Addition of a third mutation to serine at Cys490 (AMPK3CS) did not further decrease interaction with Trx1C35S, suggesting that Cys130 and Cys174 are the two major cysteines involved in the oxidative stress-induced interaction with the active site of Trx1.

AMPK2CS had markedly reduced IAM labeling at baseline and in response to H_2O_2, suggesting that Cys130 and Cys174 are also the major cysteines that undergo oxidation (Figure S5C left panel). Trx1 downregulation significantly reduced IAM labeling of AMPK in Ad-AMPKWT-transduced cardiomyocytes at baseline and further in response to GD (Figure S5C right panel), suggesting that endogenous Trx1 reduces Cys130/174. To investigate whether AMPK molecules form intermolecular disulfide bonds with each other, FLAG/HA- and myc-tagged AMPK were co-expressed in Cos7 cells and co-immunoprecipitated. FLAG-AMPKC130S-HA, in which only Cys174 is redox sensitive, was used to evaluate disulfide formation at Cys174. H_2O_2 enhanced the interaction of FLAG-AMPKC130S-HA with myc-AMPK WT, myc-AMPKC130S and myc-AMPKC174S, but not myc-AMPK2CS, and DTT abolished the effect (Figure S5D). Thus, Cys174 in one molecule forms an intermolecular disulfide bond with Cys130 or Cys174 in another molecule (Figure S5E). The H_2O_2-induced mobility shift and decreases in monomeric AMPK were partially attenuated in AMPKC130S- and AMPKC174S-transduced myocytes compared to in AMPKWT-transduced myocytes and were completely abolished in AMPK2CS-transduced myocytes (Figure 5D), suggesting that the electrophoretic mobility shift of AMPK is mediated by oxidation of Cys130 and Cys174.

To determine whether Cys130 and Cys174 in AMPK are oxidized in response to GD *in situ*, FLAG-AMPK-HA immunoprecipitated from cardiomyocytes was analyzed by quantitative mass spectrometry (MS). MMTS labeling at Cys130 and Cys174, reflecting the oxidized form, was slightly increased in the GD-treated group and significantly enhanced in the same group when endogenous Trx1 was knocked down (Figure 5E). These data suggest that Cys130 and Cys174 are oxidized in response to GD, but that endogenous Trx1 effectively attenuates this oxidation in cardiomyocytes.

Redox-Sensitive Cysteines Regulate AMPK Activity

It has been proposed that dimerization of the kinase domain of yeast Snf1, a member of the Snf1/AMPK protein family, naturally inactivates it by burying the activation segment and substrate-binding site (Nayak et al., 2006). We speculated that oxidative aggregation physically interferes with access of AMPKKs to the activation domain of AMPK, thereby inhibiting its phosphorylation and activation. To test this hypothesis, AMPK phosphorylation assays were performed with a mixture of LKB1, an AMPKK, and its regulatory subunits, STRAD and MO25, collectively termed the LKB1 complex, before and after oxidation. When phosphorylation preceded H_2O_2 treatment, AMPKα was labeled with radioactive ATP and phosphorylated AMPKα was observed at higher molecular weights after H_2O_2 treatment (Figure 6A, lanes 5–6). However, when H_2O_2 treatment preceded the kinase reaction, radioactive labeling of AMPKα was markedly attenuated (Figure 6A, lanes 7–8), suggesting that oxidized AMPK cannot be phosphorylated by AMPKK.

To elucidate the functional significance of cysteine modification in AMPK, the activities of AMPKC130S and AMPKC174S were examined. AMPKWT phosphorylation and kinase

activity were enhanced by GD (Figure 6B). However, neither AMPKC130S nor AMPKC174S was phosphorylated at Thr172 or activated in response to GD (Figure 6B). The AMPK protein levels were similar for AMPKWT, AMPKC130S and AMPKC174S, and the β2 and γ1 subunits bound to the mutants to a similar degree as to AMPKWT (Figure 6B), indicating that the mutations did not affect AMPK stability or heterotrimer complex formation. Immunofluorescent staining showed that AMPKWT, AMPKC130S and AMPKC174S were all present in both cytosol and nucleus (Figure S6A), indicating that the mutations did not affect the subcellular distribution of AMPK.

To further clarify the role of Cys130 and Cys174 in mediating AMPK activation, we generated ten different AMPKα2 mutants, in each of which a cysteine residue was replaced with a serine. Of these, only AMPKC130S and AMPKC174S failed to exhibit kinase activity in response to energy starvation in intact cells (Table S2). Although AMPKC106S exhibited a 20% reduction in kinase activity compared to WT, Cys106 oxidation was never observed, either in the MS experiments or as a change in the mobility shift pattern. The other seven mutants showed normal Thr172 phosphorylation and kinase activity. These data indicate that Cys130 and Cys174 are responsible for AMPK oxidation and are critical in the regulation of AMPK activation.

In *in vitro* kinase assays, LKB1 phosphorylated GST-AMPKWT and increased its kinase activity 6-fold. However, AMPKC130S and AMPKC174S were not phosphorylated by LKB1, and their kinase activities remained at baseline levels even in the presence of LKB1 (Figure 6C and 6D). AMPK mutants in which Cys130 or Cys174 was substituted with alanine (AMPKC130A or AMPKC174A) were not phosphorylated or activated *in vitro* or *in vivo* (Figure S6B and S6C), suggesting that structural modification of Cys130 or Cys174 inhibits AMPK activation. Similarly, AMPK irreversibly alkylated with either IAM or NEM to block free thiol groups was neither phosphorylated nor activated in the presence of LKB1 (Figure S6D and S6E). Since oxidative aggregation also prevents phosphorylation of AMPK by LKB1 (Figure 6A), these results suggest that the structural integrity of Cys130 and Cys174 is required for AMPK phosphorylation and activation. Co-immunoprecipitation experiments revealed that the physical interaction of LKB1 with AMPKWT, but not with AMPKC130S or AMPKC174S, was enhanced in response to GD (Figure 6E), suggesting that the presence of cysteines at 130 and 174 is required for assembly of the LKB1/AMPK enzyme-substrate complex and the subsequent phosphorylation/activation process during energy stress. Thus, alteration of the structure of Cys130 or Cys174 through disulfide bond-mediated oxidation, amino acid substitution or chemical alkylation blocks AMPK activation.

To further confirm that the cysteine modifications specifically affect LKB1 phosphorylation of AMPK but not the intrinsic kinase activity of AMPK, we generated constitutively active AMPK (CA-AMPK), consisting of only the kinase domain of the α2 subunit, with or without cysteine to serine mutations at amino acids 130 and 174. Addition of the C130S, C174S or 2CS mutation to CA-AMPK did not affect its kinase activity, as evidenced by phosphorylation of ACC (Figure 6F). Thus, it appears that the conserved cysteines are required for activation of WT AMPK through AMPKK-mediated phosphorylation and conformational change but not for kinase activity in CA-AMPK, which does not require activation by AMPKK.

Functional Significance of Redox-Sensitive Cysteines in AMPKα

We examined the functional effect of the CS mutants *in vitro*. Endogenous AMPKα2 in cardiomyocytes was downregulated by transduction with AMPKα2 short hairpin RNA adenovirus (Ad-sh-AMPKα2) and then reconstituted with Ad-AMPK WT or CS mutants to the same level of AMPK expression as in control myocytes (Figure S7A). AMPKα2 downregulation enhanced GD-induced cardiomyocyte death. Restoration with the WT

protein normalized GD-induced cell death to the same level as in the control group (Ad-sh-con) but reconstitution with AMPKC130S or AMPKC174S did not (Figure S7B). In addition, overexpression of either AMPKC130S or AMPKC174S attenuated GD-induced phosphorylation of PFK-2 (Figure S7C).

We next evaluated the functional significance of the CS mutations *in vivo*. Since AMPKC130S and AMPKC174S behave the same with regard to both oxidation and kinase activity, we focused on C174S. To this end, we generated two lines of transgenic mice with high and low levels of cardiac-specific expression of AMPKC174S (Tg-AMPKC174S) (Figure S7D). Expression of AMPKC174S reduced the endogenous AMPKα2 protein level, probably by destabilizing it through competition for endogenous β and γ subunit binding, and was accompanied by decreased Thr172 phosphorylation of AMPKα (Figure S7D). Tg-AMPKC174S (line 13) exhibited greater myocardial infarction than WT mice in response to ischemia (Figure 7A). Thus, intact Cys130 and Cys174 are required to promote cell survival during energy stress both *in vitro* and *in vivo*.

High-Fat Diet Enhances AMPK Oxidation

Obesity and metabolic syndrome are associated with greater cardiovascular mortality and increased susceptibility to myocardial ischemia and heart failure (Abdulla et al., 2008). We investigated whether AMPK is oxidized during metabolic stress using a mouse model of obesity (Sciarretta et al., 2012). High-fat diet (HFD) consumption by C57BL/6J mice for 18 to 20 weeks induced AMPK inactivation in the heart, accompanied by decreased Trx1 expression, AMPK cysteine oxidation, and exacerbation of myocardial infarction following prolonged ischemia (Figure 7B and 7D). However, increased Trx1 expression in Tg-Trx1 prevented AMPK oxidation and maintained AMPK activity in the heart even after HFD treatment (Figure 7C). Tg-Trx1 were also protected against the HFD-induced exacerbation of myocardial infarction (Figure 7D), suggesting that restoration of Trx1 rescues HFD-induced myocardial injury by preventing AMPK oxidation.

Discussion

We demonstrate in this study that AMPK is a critical target of Trx1 oxidoreductase activity during energy starvation. In response to energy stress, AMPK forms oxidative aggregates through intermolecular disulfide bonds at the conserved Cys130 and Cys174 residues, which inhibits phosphorylation of AMPK by AMPKK. Trx1 supports AMPK activation by reducing these key residues, acting as an essential co-factor during energy starvation (Figure S7E). However, AMPK is oxidized and cannot be activated in the presence of enhanced oxidative stress or when Trx1 activity is suppressed. Insufficient AMPK activity may contribute to the pathogenesis of metabolic disorders and enhance the risk of cardiovascular disease development, so therapeutic strategies which prevent AMPK inactivation under adverse conditions such as chronic oxidative stress and aging may prove more effective.

Identification of Novel Trx1 Targets during Myocardial Ischemia Using Trx1 Trapping Mutant

Identifying Trx1 substrates has been difficult due to the highly transient nature of the thiol disulfide exchange reaction, but substitution of Trx1 Cys35 with serine halts the reaction midway, trapping the substrate (Verdoucq et al., 1999). Although the Trx1 trapping mutant offers a convenient way to study the Trx1 regulatory network in cells, it can also detect non-physiological interacting partners, usually containing surface disulfide bonds, even if they are not redox-regulated, due to the very high reactivity of the nucleophilic Cys32 (Hisabori et al., 2005). Thus, physiological interaction between Trx1 and its potential substrates needs to be carefully evaluated.

To our knowledge, this method has not been used to identify relevant targets of Trx1 under stress *in vivo*. Using transgenic mice expressing the Trx1 trapping mutant in the heart, we were able to pull down peroxiredoxin, a well-known Trx1 substrate, confirming the validity of this genetic mouse tool. We used the mouse line with the lowest transgene expression to avoid non-specific binding. We confirmed the physical interaction between Trx1 and AMPKα using multiple methods and showed that Trx1-mediated reduction of AMPKα at Cys130 and Cys174 is essential for AMPK function in the presence of energy stress. Thus, we believe that AMPK is a physiological target of Trx1. The Trx1-trap mice, together with proteomics, detailed protein-protein interaction studies, and functional analyses, should allow us to identify additional functionally relevant Trx1 targets during other types of cardiac stress *in vivo*.

Trx1 Is a Co-factor of the AMPK Complex Necessary for its Activation

A dynamic thiol exchange reaction occurs between the Trx1 active site and AMPK cysteines in the presence of oxidative stress. However, Trx1 and AMPK interact with one another even under unstimulated conditions in cardiomyocytes. We speculate that this partially involves Trx1 domains other than the catalytic motif, since Trx1C32S/C35S still interacted with AMPK, allowing Trx1 to readily reduce AMPK when Cys130 and Cys174 are oxidized. Trx1 thus acts as an indispensable co-factor of AMPK, suppressing oxidation and supporting activation of AMPK during energy stress.

The amino acid sequences around AMPK Cys130 and Cys174 share some common features with those around cysteines in NF-κB and Ref1 known to interact with Trx1 (Qin et al., 2000). For example, the arginine at the P_{+2} position of Cys130 may be important for strong hydrophobic interaction with Trx1, and the glycine and leucine in the P_{-4} positions of Cys130 and Cys174 respectively may allow interaction with the aromatic ring of Trp31 in Trx1 (Qin et al., 2000). Both positions may help stabilize the complex between Trx1 and its substrates. Further investigation of the protein structure should clarify how Trx1 catalyzes reduction of AMPK at Cys130 and Cys174.

AMPK Is a Redox-Sensitive Kinase

Although AMPK is primarily thought of as an energy-sensitive kinase, recent studies have indicated that its activity is also regulated by oxidative stress. Several lines of evidence suggest that ROS inhibit AMPK activity (Dolinsky et al., 2009; Saberi et al., 2008) but no study has addressed whether the suppression is mediated by direct post-translational modification. Interestingly, exogenous oxidant treatment stimulates AMPK by modulating either LKB1 activity or intracellular AMP/ATP levels in some transformed cell lines (Cao et al., 2008; Han et al., 2010). We demonstrate here that ROS negatively regulate the activity of AMPK in cardiomyocytes during energy starvation through direct post-translational modification. Why is AMPK regulated differently by ROS in different cell types? We speculate that both the antioxidant level and the nature of the oxidative stress affect the overall effect of ROS upon AMPK activity. For example, the same dosage of H_2O_2 induces AMPK oxidation in cardiomyocytes but not in HEK 293 cells (Figure S4J). Compared to primary cardiomyocytes, transformed cell lines may have elevated levels of antioxidants such as Trx1 that prevent AMPK oxidation and aggregation. AMPK activity may also be regulated by distinct mechanisms under energy-sufficient and -deficient conditions. In HEK 293 cells, S-glutathiolation at Cys299 and Cys304 of AMPKα1 is essential for H_2O_2-induced AMPK activation through modulation of the auto-inhibitory domain under energy-*sufficient* conditions (Zmijewski et al., 2010). Whether Cys130 and Cys174 are modified under these conditions in HEK 293 cells is unknown, but mutation of Cys299 and Cys304 in AMPKα1 did not affect AICAR-induced AMPK activation, consistent with our observation in cardiomyocytes that neither Cys297 nor Cys302 in AMPKα2 is oxidized or involved in

energy starvation-induced AMPK activation. Thus, post-translational oxidative modifications of AMPK are stimulus-dependent.

Mutation of the redox-sensitive cysteines to serines, which in theory should mimic the reduced form, also inhibits AMPK activation, and modification of the cysteines with either chemical alkylation or via mutation abolished the interaction between AMPK and LKB1 and AMPK Thr172 phosphorylation. Thus, intact and reduced thiols at Cys130 and Cys174 are prerequisite for AMPK activation, and redox regulation at these cysteines is essential for the AMPK-mediated survival effect during energy stress. This mechanism also provides insight as to how H_2O_2 can stimulate AMPK in transformed cell lines such as HEK 293, in which a relatively high antioxidant capacity may keep Cys130 and Cys174 in the reduced form even in the presence of H_2O_2. Under such conditions, strong oxidative stress caused by exogenous H_2O_2 may allow AMPK to be activated by oxidation of another cysteine residue through some other post-translational modification, such as S-glutathiolation.

How Does Oxidation of AMPK Affect Its Structure and Kinase Activity?

Crystal structure analyses show that the yeast Snf1 kinase domain dimer is formed predominantly by hydrophobic interactions between residues within the T loop activation segment and the loop-aG region of the kinase domain (Nayak et al., 2006). The interaction at the T loop activation segment takes place around Thr210, corresponding to Thr172 in AMPK, and involves the flanking residues, including Cys212, which corresponds to Cys174 in AMPK. Although the authors predicted that van der Waals interactions play a role in mediating the dimerization, two mutations of the hydrophobic core of the dimer interface (I257E and F261E) were not sufficient to disrupt Snf1 homodimerization *in vivo*, suggesting that other mechanisms may be involved. Our results suggest that intermolecular disulfide bonds involving Cys174 may be responsible for the dimer formation in AMPK.

Snf1 dimerization buries the activation segment and substrate-binding site deep inside the dimer, representing a natural inactive form of Snf1 (Nayak et al., 2006). Our results show that oxidative modification and amino acid substitution at Cys174 or Cys130 abolish interaction between AMPK and LKB1 and Thr172 phosphorylation by LKB1. Furthermore, LKB1 cannot phosphorylate recombinant AMPK when the kinase reaction follows oxidation of AMPK *in vitro*. We speculate that the oxidative aggregate of AMPK physically interferes with access of LKB1 to the AMPK activation domain. Given that Cys130 is located on the surface of mammalian AMPK and close to the activation domain, oxidation of Cys130 in mammalian AMPK may also induce burial of the activation segment.

Since disulfide bond formation is a reversible process, it allows for tight control of AMPK activity through the balance between oxidative stress and the intact Trx1 system (Figure 4F). Indeed, Trx1-dependent reduction of AMPK is essential for AMPK activation by physiological stimuli such as energy starvation. Disulfide bond formation during AMPK oxidation can also prevent severe cysteine oxidation, which would irreversibly inhibit its kinase activity. Thus, the intermolecular disulfide bond of AMPK may also be adaptive against severe oxidative stress.

Biological Significance of AMPK as a Redox Sensor

How do myocardial ischemia and GD stimulate ROS production in cardiomyocytes? We recently showed that GD activates Nox4, a major isoform of the NADPH oxidase family that is localized on intracellular membranes (Sciarretta et al., 2013). Changes in the activity of the antioxidants and transporters controlling intracellular and mitochondrial Ca^{2+} levels may also contribute to increased ROS levels. In addition, activation of AMPK stimulates energy production pathways, including glycolysis and fatty acid oxidation, thereby

indirectly increasing mitochondrial workload and consequent electron leakage. Interestingly, AMPK plays an essential role in upregulation of Trx1 in cardiomyoctyes, which in turn prevents AMPK oxidation. AMPK activation also stimulates antioxidant capacity during energy stress (data not shown), which could be an adaptive mechanism to prevent ROS-induced damage. Thus, AMPK and Trx1 stimulate one another's activity, thereby helping to maintain the homeostasis of both energy and redox status in cardiomyocytes. We propose that AMPK has three different statuses: oxidized (inactive), reduced (activatable), and reduced and phosphorylated (active) (Figure S7E). The relative proportions of each form are determined by the intracellular energy status, the ROS level and Trx1 activity. Under physiological conditions, AMPK mainly remains in its reduced form in a Trx1-dependent manner. However, AMPK is oxidized and cannot be activated in the presence of enhanced oxidative stress or when Trx1 activity is suppressed. In our obese mouse model, we also observed decreased Trx1 protein expression. The dual effect upon Trx1 activity and Trx1 expression may explain the enhanced AMPK oxidation and inactivation in these animals. Oxidative stress has been shown to promote Trx1 degradation in vascular cells (Zschauer et al., 2011). Given that AMPK positively regulates Trx1, inhibition of AMPK may contribute to Trx1 suppression and ROS accumulation during the development of obesity or diabetes, which would further accelerate AMPK oxidation, leading to disruption of the redox and energy balances. AMPK plays a protective role in several human disorders, including myocardial ischemia, diabetes, obesity and cancers. Knowledge obtained from this investigation should be useful for the development of therapeutic strategies by which AMPK may be activated even under adverse conditions such as oxidative stress and aging.

Experimental Procedures

Transgenic Mice

Transgenic mice expressing either hTrx1C32S/C35S (Tg-Trx1C32S/C35S) or wild-type hTrx1 (Tg-Trx1) were generated on an FVB background as described previously (Yamamoto et al., 2003). Transgenic mice expressing either hTrx1C35S (Tg-Trx1C35S) or AMPKC174S (Tg-AMPKC174S) were generated on an FVB background using the α-myosin heavy chain promoter (courtesy of J. Robbins, University of Cincinnati, Cincinnati, Ohio, USA) to achieve cardiac-specific expression. Tg-Trx1 mice generated on a C57BL/6 background were used in the HFD study. All protocols concerning animal use were approved by the Institutional Animal Care and Use Committee at the New Jersey Medical School, Rutgers Biomedical and Health Sciences.

Immunoblot Analysis

Heart homogenates or cell lysates were prepared using RIPA buffer containing 50 mM Tris (pH 7.4), 150 mM NaCl, 1% Triton X-100, 0.1% SDS, 1% deoxycholic acid, 1 mM EDTA, 1 mM Na_3VO_4, 1 mM NaF, 0.5 mM 4-(2-aminoethyl) benzenesulfonyl fluoride hydrochloride, 0.5 μ/ml aprotinin, and 0.5 g/ml leupeptin. Equal amounts of proteins (10–20 μg) were subjected to SDS-PAGE. Nuclear and cytosolic fractions were prepared with NE-PER Nuclear and Cytoplasmic Extraction Reagents (Pierce). After proteins were transferred to a PVDF membrane, immunoblots were probed with the indicated antibodies. Protein abundance was analyzed densitometrically and standardized with α-tubulin or GAPDH.

For AMPK redox analysis, cardiomyocytes were incubated with ice-cold PBS containing 20 mM NEM for 15 min to block free thiol groups immediately after treatment and subsequently lysed with RIPA buffer containing 20 mM NEM to prevent further cysteine oxidation during protein extraction. Equal amounts of proteins were then subjected to SDS-PAGE with loading buffer with or without β-ME.

Immunoprecipitation

Heart homogenates or cell lysates were prepared using lysis buffer containing 50 mM Tris (pH 7.4), 150 mM NaCl, 1% Triton X-100, and 1 mM EDTA. The lysis buffer used to examine protein-protein interaction with Trx1 or its mutants was supplemented with 20 mM NEM to avoid spontaneous thiol oxidation during protein extraction or incubation. Lysates were incubated with 30 μl protein A agarose-immobilized antibody or 30 μl FLAG-agarose beads (Sigma) for 2 h at 4°C. Immuno complexes were washed with lysis buffer three times and eluted with 2X SDS sample buffer.

AMPK Kinase Assays

Immunocomplexes from Cos7 cells transfected with WT or mutant AMPK in the presence of normal or glucose-free medium were subjected to a standard AMPK kinase assay using SAMS as a substrate. One μg of *E. coli*-expressed GST-AMPKα2 (WT or mutant) was maximally activated using MgATP and AMPKK, and 5 μl of the mixture was subjected to a standard AMPK kinase assay. The phosphorylation status of AMPK was detected by autoradiography.

Detection of Thiolate Cysteines

Cardiomyocytes plated on 6 cm dishes were treated with H_2O_2 using the indicated times and doses and lysed with RIPA buffer containing 200 μM biotinylated-IAM (Sigma). The lysates were incubated with 25 μl streptavidin agarose beads (Sigma) for 2 h at 4°C. After washing with lysis buffer thr ee times, biotinylated proteins were eluted with 2X SDS sample buffer and subjected to immunoblot analysis.

Mass Spectrometry

Immunoprecipitated or *E.coli*-expressed proteins were separated by SDS-PAGE. The gel band corresponding to AMPKα2 was trypsin digested in-gel without reduction/alkylation. The resulting peptides were subjected to LC-MS/MS analysis on a U3000 LC coupled with an Orbitrap Velos tandem mass spectrometer (Thermo Fisher Scientific). MS/MS spectra were searched against a Swissprot rat database. Methionine oxidation, Cys methylthio (MMTS) and carbamidomethyl (IAM) modifications were set as variable modifications. The selected ion chromatogram peak areas of AMPKα2 peptides identified with either MMTS or IAM modifications were used for relative quantification after normalization with the average peak areas of two non-Cys-containing AMPKα2 peptides.

Statistical Analysis

All values are expressed as mean ± SEM. Statistical comparisons between groups were conducted by unpaired Student's t-test or one-way ANOVA followed by a Newman-Keuls comparison test. The value of $p<0.05$ was considered to be significant.

Supplementary Material

Refer to Web version on PubMed Central for supplementary material.

Acknowledgments

We thank Daniela Zablocki and Christopher D. Brady for critical reading of the manuscript. This work was supported in part by U.S. Public Health Service Grants HL67724, HL91469, HL102738, HL112330, and AG23039 (JS), and the Foundation of Leducq Transatlantic Network of Excellence (JS). The Orbitrap mass spectrometer used in this study is supported in part by NIH grant NS046593 (HL) for the support of a New Jersey Medical School Cancer Center Neuroproteomics Core Facility, Rutgers Biomedical and Health Sciences.

References

Abdulla J, Kober L, Abildstrom SZ, Christensen E, James WPT, Torp-Pedersen C. Impact of obesity as a mortality predictor in high-risk patients with myocardial infarction or chronic heart failure: a pooled analysis of five registries. Eur Heart J. 2008; 29:594–601. [PubMed: 18270214]

Ago T, Liu T, Zhai P, Chen W, Li H, Molkentin JD, Vatner SF, Sadoshima J. A redox-dependent pathway for regulating class II HDACs and cardiac hypertrophy. Cell. 2008; 133:978–993. [PubMed: 18555775]

Arner ES, Bjornstedt M, Holmgren A. 1-Chloro-2,4-dinitrobenzene is an irreversible inhibitor of human thioredoxin reductase. Loss of thioredoxin disulfide reductase activity is accompanied by a large increase in NADPH oxidase activity. J Biol Chem. 1995; 270:3479–3482. [PubMed: 7876079]

Berndt C, Lillig CH, Holmgren A. Thiol-based mechanisms of the thioredoxin and glutaredoxin systems: implications for diseases in the cardiovascular system. Am J Physiol Heart Circ Physiol. 2007; 292:H1227–1236. [PubMed: 17172268]

Cao C, Lu S, Kivlin R, Wallin B, Card E, Bagdasarian A, Tamakloe T, Chu WM, Guan KL, Wan Y. AMP-activated protein kinase contributes to UV- and H2O2-induced apoptosis in human skin keratinocytes. J Biol Chem. 2008; 283:28897–28908. [PubMed: 18715874]

Dolinsky VW, Chan AY, Robillard Frayne I, Light PE, Des Rosiers C, Dyck JR. Resveratrol prevents the prohypertrophic effects of oxidative stress on LKB1. Circulation. 2009; 119:1643–1652. [PubMed: 19289642]

Finkel T. Oxidant signals and oxidative stress. Curr Opin Cell Biol. 2003; 15:247–254. [PubMed: 12648682]

Fu C, Wu C, Liu T, Ago T, Zhai P, Sadoshima J, Li H. Elucidation of thioredoxin target protein networks in mouse. Mol Cell Proteomics. 2009; 8:1674–1687. [PubMed: 19416943]

Han Y, Wang Q, Song P, Zhu Y, Zou MH. Redox regulation of the AMP-activated protein kinase. PLoS One. 2010; 5:e15420. [PubMed: 21079763]

Hardie DG. Role of AMP-activated protein kinase in the metabolic syndrome and in heart disease. FEBS Lett. 2008; 582:81–89. [PubMed: 18022388]

Hawley SA, Davison M, Woods A, Davies SP, Beri RK, Carling D, Hardie DG. Characterization of the AMP-activated protein kinase kinase from rat liver and identification of threonine 172 as the major site at which it phosphorylates AMP-activated protein kinase. J Biol Chem. 1996; 271:27879–27887. [PubMed: 8910387]

Hisabori T, Hara S, Fujii T, Yamazaki D, Hosoya-Matsuda N, Motohashi K. Thioredoxin affinity chromatography: a useful method for further understanding the thioredoxin network. J Exp Bot. 2005; 56:1463–1468. [PubMed: 15851412]

Kallis GB, Holmgren A. Differential reactivity of the functional sulfhydryl groups of cysteine-32 and cysteine-35 present in the reduced form of thioredoxin from Escherichia coli. J Biol Chem. 1980; 255:10261–10265. [PubMed: 7000775]

Kuster GM, Pimentel DR, Adachi T, Ido Y, Brenner DA, Cohen RA, Liao R, Siwik DA, Colucci WS. alpha-adrenergic receptor-stimulated hypertrophy in adult rat ventricular myocytes is mediated via thioredoxin-1-sensitive oxidative modification of thiols on Ras. Circulation. 2005; 111:1192–1198. [PubMed: 15723974]

Lillig CH, Holmgren A. Thioredoxin and related molecules--from biology to health and disease. Antioxid Redox Signal. 2007; 9:25–47. [PubMed: 17115886]

Mustacich D, Powis G. Thioredoxin reductase. The Biochemical journal. 2000; 346(Pt 1):1–8. [PubMed: 10657232]

Nayak V, Zhao K, Wyce A, Schwartz MF, Lo WS, Berger SL, Marmorstein R. Structure and dimerization of the kinase domain from yeast Snf1, a member of the Snf1/AMPK protein family. Structure. 2006; 14:477–485. [PubMed: 16531232]

Oakhill JS, Steel R, Chen ZP, Scott JW, Ling N, Tam S, Kemp BE. AMPK Is a Direct Adenylate Charge-Regulated Protein Kinase. Science. 2011; 332:1433–1435. [PubMed: 21680840]

Qin J, Yang Y, Velyvis A, Gronenborn A. Molecular views of redox regulation: three-dimensional structures of redox regulatory proteins and protein complexes. Antioxid Redox Signal. 2000; 2:827–840. [PubMed: 11213487]

Reznick RM, Zong H, Li J, Morino K, Moore IK, Yu HJ, Liu ZX, Dong J, Mustard KJ, Hawley SA, et al. Aging-associated reductions in AMP-activated protein kinase activity and mitochondrial biogenesis. Cell Metab. 2007; 5:151–156. [PubMed: 17276357]

Russell RR 3rd, Li J, Coven DL, Pypaert M, Zechner C, Palmeri M, Giordano FJ, Mu J, Birnbaum MJ, Young LH. AMP-activated protein kinase mediates ischemic glucose uptake and prevents postischemic cardiac dysfunction, apoptosis, and injury. J Clin Invest. 2004; 114:495–503. [PubMed: 15314686]

Saberi B, Shinohara M, Ybanez MD, Hanawa N, Gaarde WA, Kaplowitz N, Han D. Regulation of H(2)O(2)-induced necrosis by PKC and AMP-activated kinase signaling in primary cultured hepatocytes. Am J Physiol-Cell Ph. 2008; 295:C50–C63.

Saitoh M, Nishitoh H, Fujii M, Takeda K, Tobiume K, Sawada Y, Kawabata M, Miyazono K, Ichijo H. Mammalian thioredoxin is a direct inhibitor of apoptosis signal-regulating kinase (ASK) 1. Embo J. 1998; 17:2596–2606. [PubMed: 9564042]

Sciarretta S, Zhai P, Shao D, Maejima Y, Robbins J, Volpe M, Condorelli G, Sadoshima J. Rheb is a critical regulator of autophagy during myocardial ischemia: pathophysiological implications in obesity and metabolic syndrome. Circulation. 2012; 125:1134–1146. [PubMed: 22294621]

Sciarretta S, Zhai P, Shao D, Zablocki D, Nagarajan N, Terada LS, Volpe M, Sadoshima J. Activation of Nox4 in the Endoplasmic Reticulum Promotes Cardiomyocyte Autophagy and Survival During Energy Stress Through the PERK/eIF-2alpha/ATF4 Pathway. Circ Res. 2013

Sriwijitkamol A, Coletta DK, Wajcberg E, Balbontin GB, Reyna SM, Barrientes J, Eagan PA, Jenkinson CP, Cersosimo E, DeFronzo RA, et al. Effect of acute exercise on AMPK signaling in skeletal muscle of subjects with type 2 diabetes: a time-course and dose-response study. Diabetes. 2007; 56:836–848. [PubMed: 17327455]

Tao L, Gao E, Bryan NS, Qu Y, Liu HR, Hu A, Christopher TA, Lopez BL, Yodoi J, Koch WJ, et al. Cardioprotective effects of thioredoxin in myocardial ischemia and reperfusion: role of S-nitrosation [corrected]. Proc Natl Acad Sci U S A. 2004; 101:11471–11476. [PubMed: 15277664]

Verdoucq L, Vignols F, Jacquot JP, Chartier Y, Meyer Y. In vivo characterization of a thioredoxin h target protein defines a new peroxiredoxin family. Journal of Biological Chemistry. 1999; 274:19714–19722. [PubMed: 10391912]

Yamamoto M, Yang G, Hong C, Liu J, Holle E, Yu X, Wagner T, Vatner SF, Sadoshima J. Inhibition of endogenous thioredoxin in the heart increases oxidative stress and cardiac hypertrophy. J Clin Invest. 2003; 112:1395–1406. [PubMed: 14597765]

Zmijewski JW, Banerjee S, Bae H, Friggeri A, Lazarowski ER, Abraham E. Exposure to hydrogen peroxide induces oxidation and activation of AMP-activated protein kinase. J Biol Chem. 2010; 285:33154–33164. [PubMed: 20729205]

Zschauer TC, Kunze K, Jakob S, Haendeler J, Altschmied J. Oxidative Stress-Induced Degradation of Thioredoxin-1 and Apoptosis Is Inhibited by Thioredoxin-1-Actin Interaction in Endothelial Cells. Arterioscl Throm Vas. 2011; 31:650–U370.

Highlights

- The AMPKα subunit is a direct substrate of Trx1.
- Oxidation of Cys130 and Cys174 induces aggregation of AMPKα.
- Oxidation of AMPK prevents activation and phosphorylation by AMPK kinases.
- Trx1-mediated reduction of Cys130 and Cys174 is essential for AMPK function.

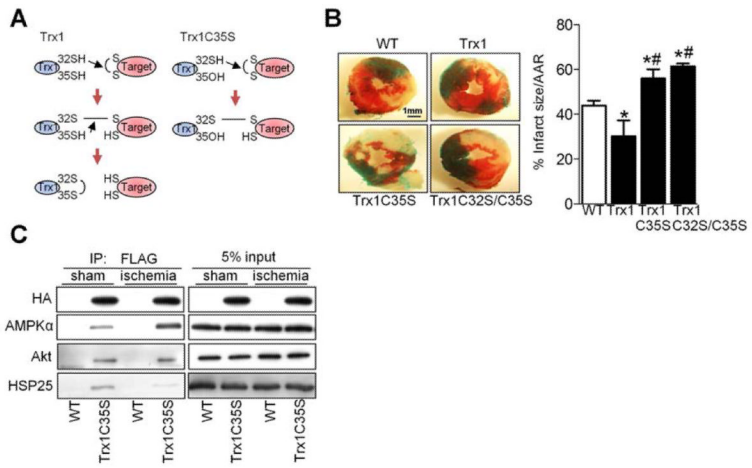

Figure 1. Identifying AMPKα as a Trx1 Substrate during Myocardial Ischemia

(A) The principle of trapping Trx1 substrates. Left panel shows normal reduction of a disulfide bond by Trx1. Right panel shows trapping of a protein with a disulfide bond by the Trx1 trapping mutant (Trx1C35S), in which the second cysteine in the CXXC active site has been replaced by serine. Trx1C35S forms a mixed disulfide bond with the target protein. The resulting complex can be purified and the trapped protein identified by immunoblot analysis. (B) Tg-Trx1, Tg-Trx1C35S, Tg-Trx1C32S/C35S and control WT mice were subjected to ischemia for 3 h. The myocardial infarct area/area at risk (% infarct size/AAR) is shown (*$p<0.05$ vs. WT, #$p<0.05$ vs. Tg-Trx1, n=4-6). (C) Tg-Trx1C35S and WT mice were subjected to ischemia for 20 min. Homogenates prepared from sham-operated hearts and ischemic areas were used for co-immunoprecipitation and immunoblots for the indicated molecules were performed. Error bars represent SEM.

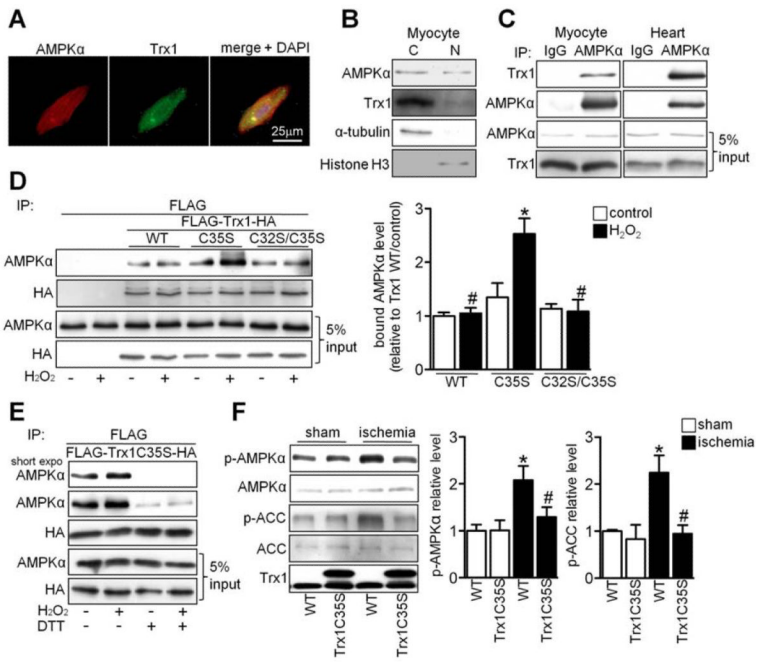

Figure 2. AMPK Interacts with the Active Site of Trx1

(A) Myocytes were stained with AMPKα antibody (red), Trx1 antibody (green) and DAPI (blue). (B) The presence of AMPKα and Trx1 was examined in cytosolic and nuclear fractions prepared from neonatal cardiomyocytes. (C) Interaction between AMPKα and Trx1 was examined. Results are representative of three individual experiments. (D-E) Cos7 cells were transfected with N-terminal FLAG and C-terminal HA tagged Trx1 WT (FLAG-Trx1-HA) or mutant plasmids. (D) Cells transfected with the indicated plasmids were treated with or without 100 μM H_2O_2 for 30 min. Interaction between AMPKα and Trx1 mutants was examined. Statistical analysis of the immunoblot densitometric measurements is shown (*p<0.05 vs. WT/H_2O_2, #p<0.05 vs. C35S/H_2O_2, n=3). (E) Cells transfected with the indicated plasmids were treated with or without 100 μM H_2O_2 for 30 min and lysed with or without 1 mM DTT. Immunoblots with AMPKα and HA antibodies are shown. (F) Tg-Trx1C35S and WT mice were subjected to ischemia for 20 min. Homogenates prepared from sham-operated hearts and the ischemic areas were used for immunoblot analyses of p-AMPKα, AMPKα, p-ACC, ACC, and Trx1. Statistical analyses of densitometric measurements of p-AMPKα and p-ACC are shown (*p<0.05 vs. WT/sham, #p<0.05 vs. WT/ischemia, n=3-5). Error bars represent SEM.

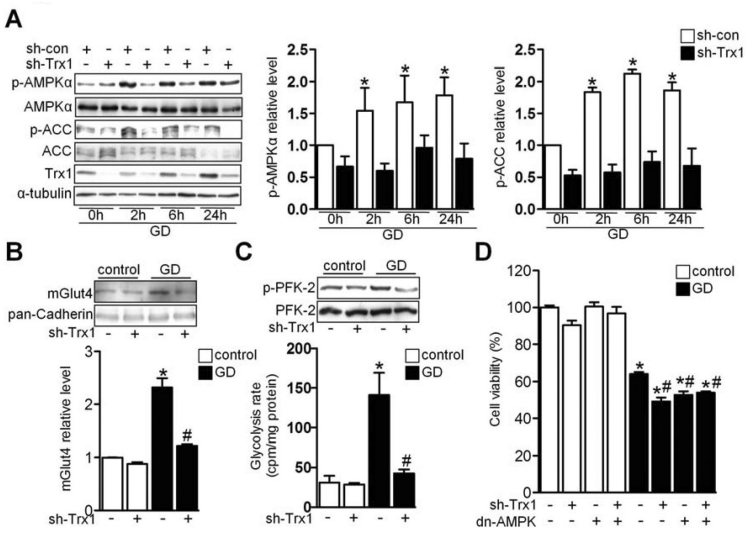

Figure 3. Trx1 Is an Essential Co-factor for AMPK Activation during Energy Stress

(A) Cardiomyocytes transduced with the indicated adenovirus were incubated with glucose-free medium for the indicated times. Cell lysates were analyzed by immunoblot for p-AMPKα, AMPKα, p-ACC, ACC, Trx1, and α-tubulin. Statistical analyses of densitometric measurements of p-AMPKα and p-ACC are shown (*p<0.05 vs. sh-con/0 h, n=3). (B-D) Cardiomyocytes transduced with the indicated adenovirus were incubated with normal or glucose-free medium. (B) Subcellular fractionation was performed to examine membrane Glut4 expression. Statistical analysis of densitometric measurement of membrane Glut4 is shown (*p<0.05 vs. control, #p<0.05 vs. GD, n=3). (C) Lysates were analyzed by immunoblot for p-PFK-2 and PFK-2. Results are representative of 3 individual experiments. Glycolysis rate was examined (*p<0.05 vs. control, #p<0.05 vs. GD, n=3). (D) Cell viability was measured (*p<0.05 vs. control, #p<0.05 vs. GD, n=3). Error bars represent SEM.

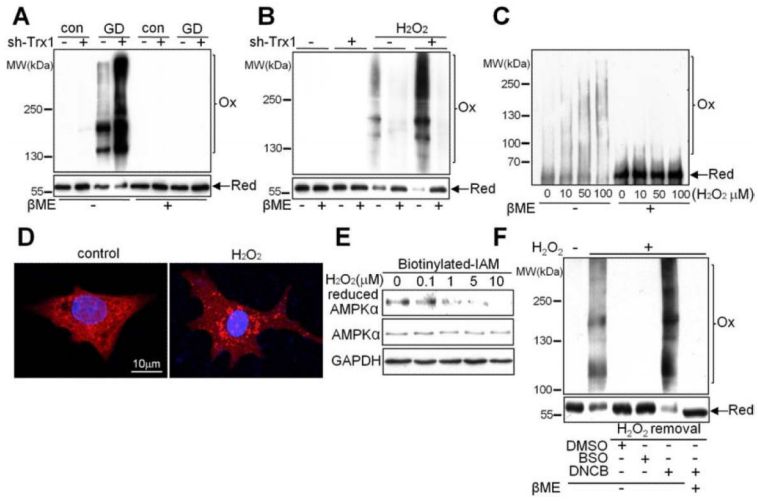

Figure 4. AMPK Is Oxidized and Forms Intermolecular Disulfide Bonds during Energy Stress

(A-B) AMPK oxidation was examined. Cardiomyocytes transduced with the indicated adenovirus were incubated with or without glucose (A) or H_2O_2 (B). Lysates were analyzed by immunoblot with an AMPKα antibody under reducing or non-reducing conditions. Duplicate samples were run on 6% and 8% gels to present the oxidized and reduced forms of AMPK, respectively. Molecular weights, as determined by a simultaneously-run protein ladder, are shown. In most of the following figures, the oxidized and reduced forms of AMPK are presented as described above. Results are representative of 3 individual experiments. (C) Recombinant AMPKα2 was incubated with H_2O_2 at the indicated concentrations for 10 min and AMPK oxidation was examined. Results are representative of 3 individual experiments. (D) Cardiomyocytes were treated with or without 100 μM H_2O_2 for 10 min and stained with AMPKα antibody (red) and DAPI (blue). (E) Cardiomyocytes were treated with H_2O_2 at the indicated concentrations for 10 min. The extent of cysteine reduction in AMPKα was detected. Results are representative of 3 individual experiments. (F) Reduction of AMPKα depends upon the Trx1 system. Cardiomyocytes were preincubated with 100 μM BSO for 24 h or 100 μM DNCB for 15 min and then treated with H_2O_2 for 30 min to oxidize AMPK. The medium was replaced with H_2O_2-free medium containing DMSO alone or DMSO with either BSO (100 μM) or DNCB (100 μM) for another 60 min. AMPK oxidation was examined as previously described. Results are representative of 3 individual experiments.

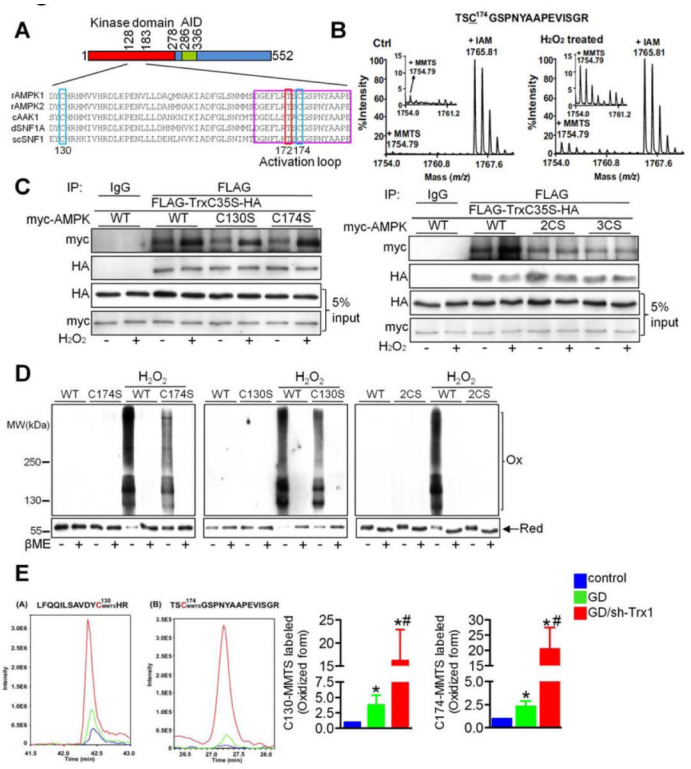

Figure 5. Conserved Cysteines Participate in the Intermolecular Disulfide Bond Formation in AMPK

(A) Amino acid alignment of the AMPK family kinase domain (amino acids 128-183 in Rat AMPKα2). The positions of conserved cysteine residues corresponding to Cys130 and Cys174 in rat AMPKα2 are indicated by blue rectangles. The conserved phosphorylation site corresponding to Thr172 in AMPKα2 is indicated by a red rectangle. The activation loop of AMPKα is indicated by a purple rectangle. (B) The MS spectra of AMPKα2 peptide [172-188]. The peptide in the control group contained MMTS-modified Cys174 (m/z 1754.79, corresponding to oxidized thiol) as well as IAM-modified Cys174 (m/z 1765.81, corresponding to reduced thiol). In the H_2O_2-treated group, the intensity of the peak corresponding to oxidized Cys174 was increased. (C) Cos7 cells transfected with FLAG-Trx1C35S-HA and Myc-tagged AMPK WT or mutant plasmids were treated with or without 100 μM H_2O_2 for 30 min. Interaction between AMPK and the Trx1C35S trapping mutant was evaluated with immunoblot analyses. Results are representative of 3 individual experiments. (D) Cardiomyocytes transduced with the indicated adenoviruses harboring C-terminal HA-tagged AMPK were incubated with or without H_2O_2 for 30 min. The effect of mutation of AMPK on its oxidation was examined. (E) Cardiomyocytes transduced with N-terminal FLAG- and C-terminal HA-tagged AMPK (FLAG-AMPK-HA) adenovirus were incubated with glucose-free medium for 2 h in the presence or absence of Ad-sh-Trx1. Lysates were prepared in the presence of 100 mM IAM to label reduced cysteines. Oxidized cysteines were reduced with TCEP followed by MMTS alkylation. Samples were then immunoprecipitated with anti-FLAG agarose beads and immunoprecipitates were analyzed by MS. The overlay extract ion chromatograms of peptides LFQQILSAVDYC_{MMTS}HR (A), corresponding to oxidized C130, and TSC_{MMTS}GSPNYAAPEVISGR (B), corresponding to oxidized C174, in control (blue line), GD (green line) and GD plus Ad-sh-Trx1 (red line) samples are shown. Ratios of the oxidized peptide peak heights relative to those of the control groups are also shown (*p<0.05 vs. control, #p<0.05 vs. GD, n=5). Error bars represent SEM.

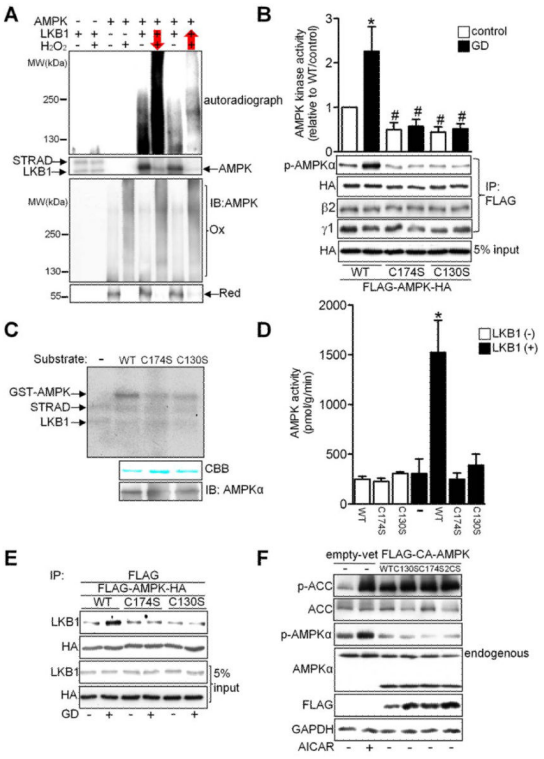

Figure 6. Intact Cysteine Residues Are Required for LKB1-Mediated Phosphorylation of AMPK

(A) Recombinant AMPKα2 was incubated with LKB1 complex and H_2O_2, with arrows indicating the order of treatment. AMPK phosphorylation and oxidation were detected by autoradiography and immunoblot with an AMPKα antibody, respectively. Results are representative of 3 individual experiments. (B) Cos7 cells transfected with either FLAG-AMPK WT-HA or the indicated mutants were incubated with glucose-free medium for 2 h. After immunoprecipitation with anti-FLAG agarose beads, levels of AMPKα Thr172 phosphorylation and of bound AMPK β2 and γ1 subunits were evaluated. Alternatively, the immunocomplex was subjected to AMPK kinase assay (*$p<0.05$ vs. WT/control, #$p<0.05$ vs. WT/GD, n=3). (C-D) GST-AMPKα2 WT or mutants were incubated with LKB1 complex. (C) AMPK phosphorylation was detected by autoradiography. Coomassie brilliant blue (CBB) dye staining and anti-AMPKα immunoblot of the recombinant substrates are also shown. (D) Standard AMPK kinase assays were performed using SAMS peptide as a substrate (*$p<0.05$ vs. WT/LKB1(-), n=3). (E) Cos7 cells transfected with either FLAG-AMPK WT-HA or the indicated mutants were incubated with glucose-free medium for 30 min. Interaction between LKB1 and AMPK was examined. Results are representative of 3 individual experiments. (F) Cos7 cells transfected with the indicated plasmids were analyzed by immunoblot for p-ACC, ACC, p-AMPKα, AMPKα, FLAG, and GAPDH. AICAR treatment was used as a positive control. Results are representative of 3 individual experiments. Error bars represent SEM.

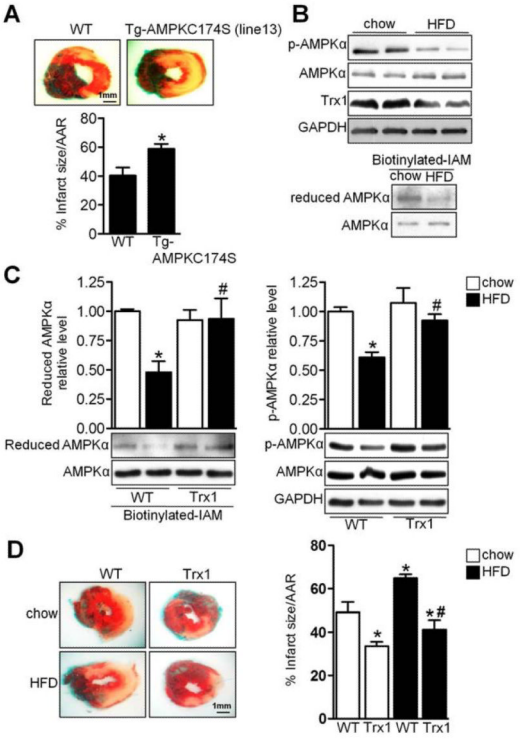

Figure 7. HFD Induced AMPK Oxidation *in Vivo*

(A) Tg-AMPKC174S and WT mice were subjected to ischemia for 3 h. Myocardial infarct area/area at risk (% infarct size/AAR) is shown (*p<0.05 vs. WT, n=7). (B–C) Tg-Trx1 and WT mice on C57BL/6J background were fed chow or HFD for 20 weeks. Heart lysates were analyzed by immunoblot for p-AMPKα, AMPKα, Trx1, and GAPDH. The extent of AMPKα cysteine reduction was analyzed. Statistical analyses of densitometric measurements of reduced AMPKα and p-AMPKα are shown (*p<0.05 vs. WT/chow, #p<0.05 vs. WT/HFD, n=3–4). (D) Tg-Trx1 and WT mice were fed chow or HFD for 20 weeks and subjected to ischemia for 3 h. Myocardial infarct area/area at risk (% infarct size/ARR) is shown (*p<0.05 vs. WT/chow, #p<0.05 vs. WT/HFD, n=5). Error bars represent SEM.